TERM

ORIGINAL ARTICLE

Induced Intermediate Mesoderm Combined with Decellularized Kidney Scaffolds for Functional Engineering Kidney

Jianye Zhang[1] · Kailin Li[2] · Feng Kong[2,3,4] · Chao Sun[2] · Denglu Zhang[5] ·
Xin Yu[1] · Xuesheng Wang[1] · Xian Li[6] · Tongyan Liu[6] · Guangfeng Shao[1] ·
Yong Guan[1,7] · Shengtian Zhao[1,3,4,7]

Abstract

BACKGROUND: Chronic kidney disease is a severe threat to human health with no ideal treatment strategy. Mature mammalian kidneys have a fixed number of nephrons, and regeneration is difficult once they are damaged. For this reason, developing an efficient approach to achieve kidney regeneration is necessary. The technology of the combination of decellularized kidney scaffolds with stem cells has emerged as a new strategy; however, in previous studies, the differentiation of stem cells in decellularized scaffolds was insufficient for functional kidney regeneration, and many problems remain.

METHODS: We used 0.5% sodium dodecyl sulfate (SDS) to produce rat kidney decellularized scaffolds, and induce adipose-derived stem cells (ADSCs) into intermediate mesoderm by adding Wnt agonist CHIR99021 and FGF9 *in vitro*. The characteristics of decellularized scaffolds and intermediate mesoderm induced from adipose–derived stem cells were identified. The scaffolds were recellularized with ADSCs and intermediate mesoderm cells through the renal artery and ureter. After cocultured for 10 days, cells adhesion and differentiation was evaluated.

RESULTS: Intermediate mesoderm cells were successfully induced from ADSCs and identified by immunofluorescence and Western blotting assays (OSR1 + , PAX2 +). Immunofluorescence showed that intermediate mesoderm cells differentiated into tubular-like (E-CAD + , GATA3 +) and podocyte-like (WT1 +) cells with higher differentiation efficiency than ADSCs in the decellularized scaffolds. Comparatively, this phenomenon was not observed in induced intermediate mesoderm cells cultured *in vitro*.

CONCLUSION: In this study, we demonstrated that intermediate mesoderm cells could be induced from ADSCs and that they could differentiate well after cocultured with decellularized scaffolds.

Keywords Kidney regeneration · Decellularized scaffolds · Adipose-derived stem cells · Intermediate mesoderm cells · Induced differentiation

✉ Yong Guan
guanyongsdu@163.com

✉ Shengtian Zhao
zhaoshengtian@sdu.edu.cn

1 Department of Urology, The Second Hospital, Shandong University, 247 Beiyuan Street, Jinan 250033, Shandong, People's Republic of China

2 Department of Central Research Lab, The Second Hospital, Shandong University, 247 Beiyuan Street, Jinan 250033, Shandong, People's Republic of China

3 Key Laboratory for Kidney Regeneration of Shandong Province, 247 Beiyuan Street, Jinan 250033, Shandong, People's Republic of China

4 Shandong University- Karolinska Institutet Collaborative Laboratory for Stem Cell Research, 247 Beiyuan Street, Jinan 250033, Shandong, People's Republic of China

5 The Affiliated Hospital of Shandong University of Traditional Chinese Medicine, 16369 Jingshi Road, Jinan 250011, Shandong, People's Republic of China

1 Introduction

End-stage renal disease (ESRD) is a leading cause of death worldwide. Approximately 2.618 million people received renal replacement therapy (RRT) in 2010, and an estimated 2.284 million people might have died if RRT was not available. By 2030, the number of patients receiving RRT will reach 5.439 million [1]. The main treatments for ESRD are dialysis and kidney transplantation, but both methods have disadvantages. Dialysis can affect the quality of life and may lead to cardiovascular or other diseases. Kidney transplantation is the ideal treatment for ESRD, but immune rejection and a shortage of donor kidneys restrict its widespread application [2–4]. Thus, the need to find new ways to treat ESRD is urgent.

Kidney regeneration is aimed at building a new kidney with renal structures and functions. Many methods for achieving kidney regeneration exist [5] and include the use of decellularized scaffolds [6], blastocyst complementation [7], metanephros transplantation [8], kidney organoids [9], and bioartificial kidneys [10]. The combination of decellularized (DC) kidney scaffolds with stem cells for kidney regeneration is a newly developed strategy [11, 12]. DC scaffolds retain a normal kidney structure and extracellular factors without the cellular components. Because donor cells are eluted during the preparation of the decellularized scaffolds, their immunogenicity is greatly decreased. The DC scaffolds retained kidney extracellular matrix (ECM) and the natural structure after decellularization [13], and the complete vascular system could support endothelial cells well. Moreover, supplying nutrition is convenient for transplantation *in vivo* or *in vitro*. The scaffolds retained location-specific proteins, which could guide stem cell adhesion, migration and differentiation, and the retained vasculature could be repopulated and utilized for equal distribution of media and nutrients. A recent study demonstrated that DC kidney scaffolds could induce embryonic stem cell-derived metanephric mesenchyme differentiation into renal cells [14].

Recent studies have shown that embryonic stem cells (ESCs) or human induced pluripotent stem cells (hiPSCs) seeded into DC scaffolds could differentiate into partial kidney structures with incomplete kidney function [15]; however, their adhesion and differentiation were unsatisfactory [16, 17], and the use of ESCs is limited because of ethical considerations. Adipose-derived stem cells (ADSCs) were first described in 2002 by Zuk et al. [18]. They are obtained easily and have the capacity to differentiate in multiple cell lineages [19–21].

Sambi et al. showed that while undifferentiated ESCs could grow in DC scaffolds, differentiation was limited. In contrast, when stem cells were induced into kidney progenitor cells and combined with a DC scaffold, the cells could further differentiate into renal cells [14]. The same problems occurred in our previous studies on the adhesion and differentiation of stem cells [22, 23]. Takasato et al. induced hiPSCs *in vitro* to obtain kidney organoids that possessed kidney structures and partial kidney function [9], but because of a lack of blood supply, the kidney progenitor cells were limited in their growth and functional differentiation.

In this study, we induced intermediate mesoderm (IM) cells from ADSCs *in vitro* and then seeded the IM cells into DC scaffolds through the ureter and renal artery to engineer a regenerative kidney. The differentiation of the seeded cells and the kidney structure were compared. We speculated that DC scaffolds play an important role as biomaterials in the induction of stem cell differentiation to achieve kidney regeneration.

2 Materials and methods

2.1 Isolation and culture of primary ADSCs

ADSCs were prepared as previously described [18, 24]. After anesthetizing the rats, the inguinal fat pad was removed and washed with phosphate-buffered saline (PBS) to eliminate residual blood cells and tissue debris. After the fat pad volume was recorded, an equal volume of 0.1% collagenase I was added, and the adipose tissue was digested at 37 °C in an air bath shaker for 30 min. The digested tissue was then allowed to stand for 5 min. Thereafter, the undigested adipose tissue was discarded. The lower cell suspension was centrifuged at 1500 rpm for 10 min, and the supernatant was discarded to obtain the adipose stem cell mass at the bottom of the tube. The cells were finally resuspended in medium, adjusted to a density of 1×10^5/mL, and inoculated in a cell culture flask.

2.2 Osteogenic, adipogenic and chondrogenic induction

ADSCs at passage 4 were seeded on 6-well plates at a concentration of 1×10^5/mL. When the cells reached 80% confluence, adipogenic induction medium (Dulbecco's modified Eagle medium (DMEM)/F12 containing 10% fetal bovine serum (FBS), 1 µmol/L dexamethasone, 10 µmol/L insulin, 200 µmol/L indomethacin, and

6   The Second Hospital of Shandong University, 247 Beiyuan Street, Jinan 250033, Shandong, People's Republic of China

7   Shandong Provincial Hospital of Shandong University, 324 Jingwuweiqi Road, Jinan 250021, Shandong, People's Republic of China

0.5 mmol/L isobutylmethylxanthine) was added for 14 days to induce adipogenic differentiation, and Oil Red O staining was performed to observe the results. For osteogenesis induction, osteogenic induction medium (DMEM/F12 containing 10% FBS, 0.1 µmol/L dexamethasone, 50 µmol/L ascorbate-2-phosphate, and 10 mmol/L β-glycerol phosphate) was added. After 21 days, alizarin red staining was performed to assess osteoblastic induction. For chondrogenic induction, ADSCs were adjusted to a concentration of 5×10^5/ml. The cell suspension was added to 15 ml polypropylene culture tubes in aliquots of 0.5 ml and centrifuged. The supernatant was not aspirated, and the pellet was not resuspended. Finally, the cells were treated with chondrogenic induction medium (L-DMEM/F12, 10% FBS, 10 µg/L TGF-β3, 0.1 µmol/L dexamethasone, 50 µmol/L vitamin C, 6.25 mg/L insulin) for 21 days for differentiation into chondrocytes. The differentiated cells were identified by Toluidine Blue staining to observe the results.

2.3 Flow cytometry of ADSCs

Flow cytometry (TIANGEN, Beijing, China) was carried out to analyze specific surface antigens on ADSCs using antibodies against CD29, CD90, CD105, CD34, and CD45 [25, 26]. ADSCs at passage 4 were washed three times with PBS, and the cells were harvested with 0.25% trypsin/ethylenediaminetetraacetic acid (EDTA). After digestion, the cells were centrifuged at 1000 rpm for 5 min, washed twice with PBS, and resuspended at 1×10^6 cells/mL for antibody staining. Unstained cells were used as negative controls.

2.4 Kidney harvest and preparation of DC scaffolds

The kidney scaffold was prepared according to our previous protocol [27]. Briefly, thirty Wistar rats, weighing approximately 220–300 g (Animal Center of Shandong University, Jinan, China), were anesthetized with chloral hydrate. A longitudinal abdominal incision was made, and the kidney was isolated and harvested after the renal artery, vein, and ureter were transected. The renal artery was catheterized with a 24-gauge cannula (Xinhua Medical, Zibo, China), and the ureter was catheterized with a 26-gauge cannula. The kidney was connected to a peristaltic pump (Baoding Longer Precision Pump Co., Baoding, China) and perfused with $1 \times$ PBS to remove residual blood, and 0.5% sodium dodecyl sulfate solution (SDS) was used to decellularize the kidney at 250 µL/min. After 6 h, the DC scaffolds became transparent and were perfused with sterile $1 \times$ PBS for 24 h to remove residual SDS.

2.5 DNA quantification

A TIANamp genomic DNA kit was used to quantify the DNA content of fresh and decellularized kidneys according to the manufacturer's instructions. Briefly, the samples were fragmented into pieces for cell suspension and centrifugation, and the precipitates were then incubated at 56 °C until completely dissolved by proteinase K and a digestion buffer. An assay was then performed in convenient spin-column format according to the manufacturer's instructions. Finally, the extracts were characterized spectrophotometrically (NanoDrop 1000; Thermo Scientific, Waltham, MA, USA). Absorbance was measured at 260 nm to estimate the yield of nucleic acids. And the absorbance ratio at OD260/OD280 was used to estimate the purity of nucleic acids.

2.6 Collagen quantification

DC scaffolds and kidneys were used in this part of the experiment (n = 10 in each group) to quantify the collagen content of untreated and decellularized scaffolds. Lyophilized tissue samples were subjected to acid-pepsin digestion at 4 °C overnight to release tissue collagen into solution. Then, Sircol dye reagent was added to the samples, which were then mixed in a gentle mechanical shaker for 30 min and centrifuged at 12,000 rpm for 10 min. The supernatant was discarded, and an alkali reagent was added to release and recover the collagen-bound dye. The assay was then performed as instructed. All concentrations were determined by a standard curve generated in parallel, and values were normalized to the original tissue dry weight.

2.7 Growth factor assays

DC scaffolds and kidneys were used in this part of the experiment (n = 10 in each group). The cytokine levels in DC scaffolds and normal kidneys were measured using enzyme-linked immunosorbent assay (ELISA) kits (R&D system, Minneapolis, MN, USA). Tissues were homogenized in 1 ml PBS and stored overnight at − 20 °C. After two freeze–thaw cycles, the homogenates were centrifuged. The supernatant was collected and assayed immediately according to the manufacturer's instructions. Briefly, samples were added to each well and incubated for 2 h at 37 °C. After removing the liquid from each well, biotin antibody (1X) was then added to each well, and the samples were incubated for 1 h at 37 °C. Horseradish peroxidase avidin (1X) was added to each well after washing, and the samples were incubated for another hour at 37 °C. TMB substrate was then added to each well, followed by incubation for 20 min at 37 °C before addition of the stop solution. The concentrations of vascular

ADSC

adipogenesis

osteogenesis

chondrogenic

CD29

CD90

CD105

CD34

CD45
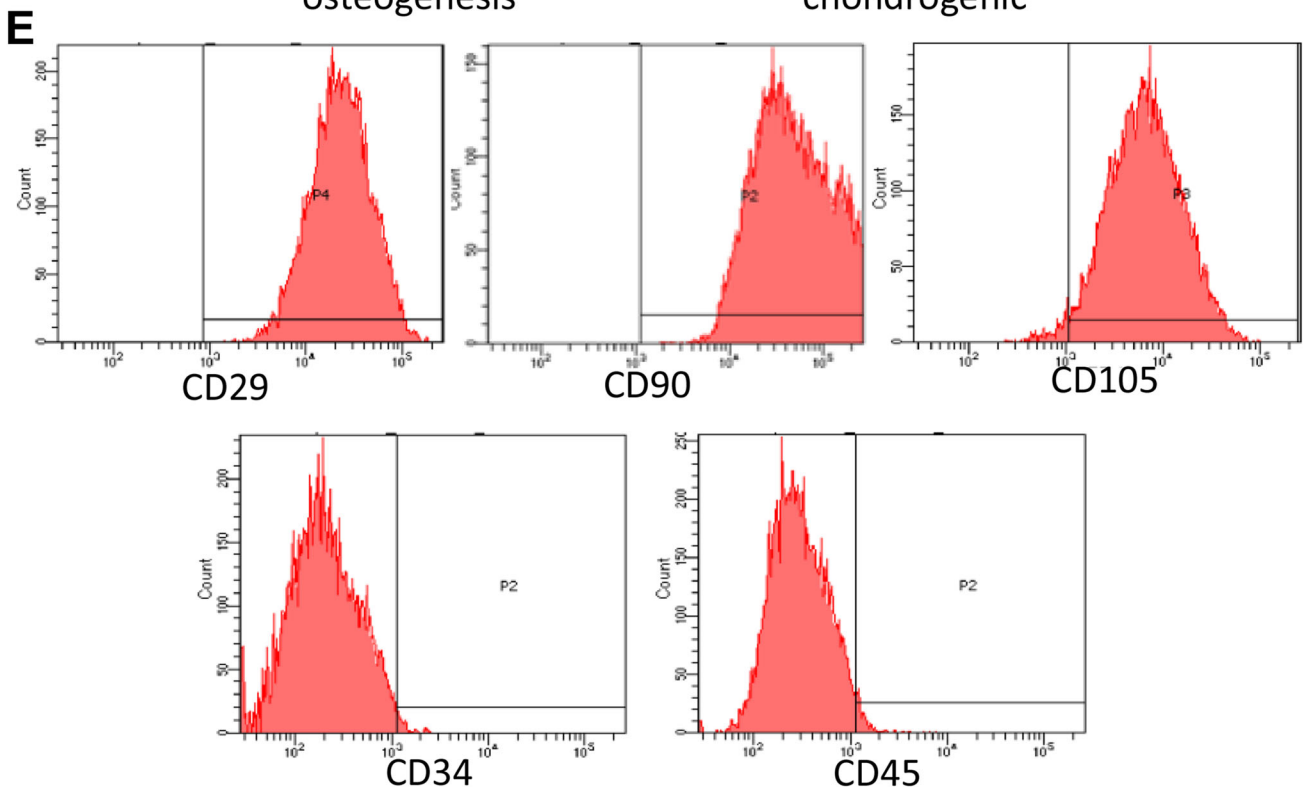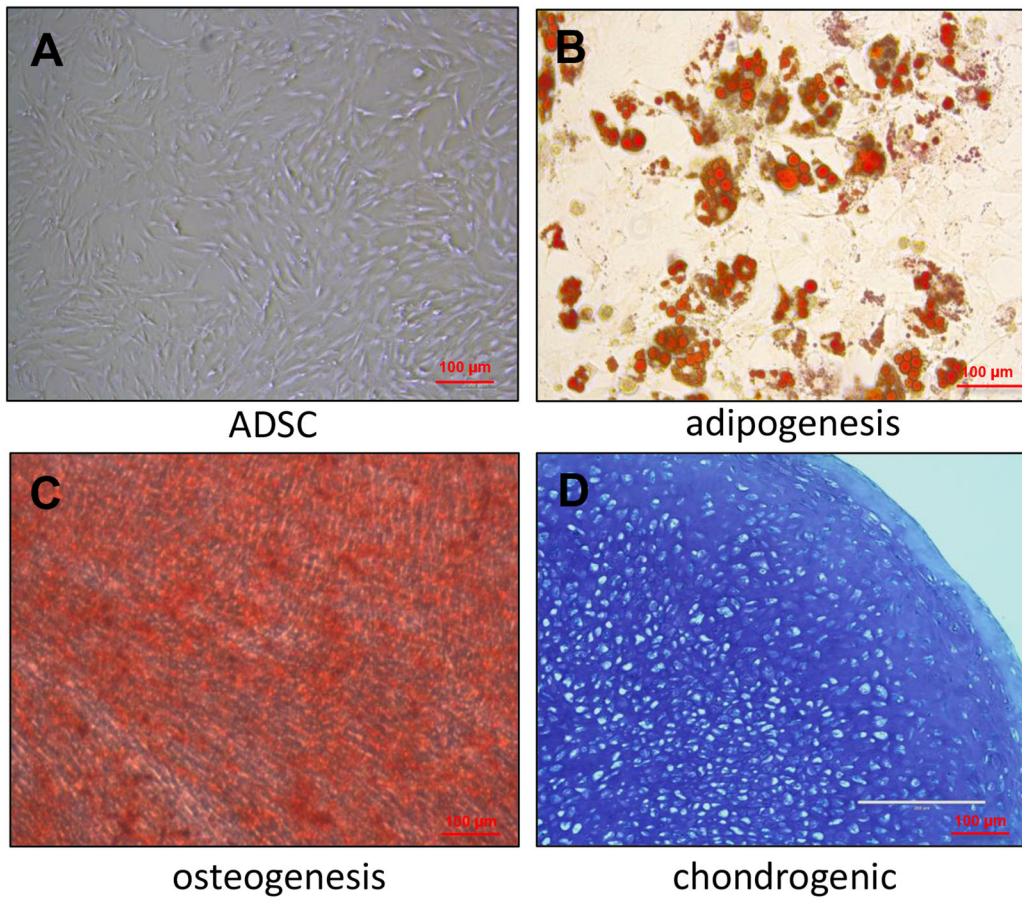
◄**Fig. 1** Identification of ADSCs. **A** Microscopic observation that most ADSCs were spindle-shaped. **B** Oil red O staining for ADSC adipogenic differentiation. **C** Alizarin red staining for ADSC osteogenic differentiation. **D** Toluidine blue staining for ADSC chondrogenic differentiation. Scale bar is 100 μm. E Surface marker analysis by flow cytometry: CD90, CD29, and CD105 were greater than 95%; CD45 and CD71 showed negative results

endothelial growth factor (VEGF), transforming growth factor (TGF)-β, and hepatocyte growth factor (HGF) were assessed with a microplate reader at 450 nm.

2.8 Histological examination

To compare kidneys and DC scaffolds, the tissues were fixed in 10% formalin, sectioned after paraffin embedding, and subjected to hematoxylin/eosin (H&E) and Masson's trichrome staining (Solarbio, Beijing, China).

2.9 Induction of ADSC differentiation into IM cells

Takasato's 7-day induction protocol was followed to induce ADSC differentiation into IM cells [28]. ADSCs were plated into a T25 flask, and when they reached approximately 40–50% confluence, medium containing 8 μM canonical Wnt agonist CHIR99021 (R&D system, Minneapolis, MN, USA) was added to induce differentiation. The medium was changed every other day for 4 days and thereafter replaced with medium containing 200 ng/mL fibroblast growth factor 9 (FGF9) (R&D system, Minneapolis, MN, USA) every other day for 3 days to induce differentiation into IM cells.

2.10 Immunofluorescence and western blotting

Immunofluorescence staining was performed to identify IM cells and the differentiation of cells in the DC scaffolds. The cells were fixed by paraformaldehyde for 1 h, permeabilized with 0.5% Triton X-100 for 30 min and blocked with 5% goat serum for 1 h. The cells were then incubated with antibodies against PAX2 and OSR1, which are specific markers of IM, incubated overnight at 4 °C, washed three times with PBS, incubated with secondary antibodies for 1 h, and subjected to nuclear counterstaining using 4,6-diamino-2-phenylindole. The same method was applied to frozen sections of recellularized scaffolds using antibodies against WT1 (a marker of podocytes), E-CAD (a marker of tubules) and GATA3 (a marker of tubules) to demonstrate differentiation. Western blotting was conducted to detect the protein expression of PAX2 and OSR1 in IM cells. IM cells and ADSCs were digested by 0.25% trypsin/EDTA (Gibco, Grand Island, NY, USA), and tissue lysates were prepared with radioimmunoprecipitation assay

buffer. Mouse embryonic tissues at day 9.5 (as a positive control), ADSCs, and IM cells were resolved by SDS–polyacrylamide gel electrophoresis and transferred to polyvinylidene difluoride membranes. The blots were then blocked with 5% bovine serum albumin at room temperature for 1 h and incubated with primary antibodies against PAX2 and OSR1 at 4 °C overnight. The blots were subsequently incubated with secondary antibody at room temperature for 1 h, and the results were visualized by an enhanced chemiluminescence system.

2.11 Recellularization of kidney scaffolds

Kidney scaffolds were recellularized according to our previous protocol [23]. Briefly, after the decellularized scaffold was prepared, ADSCs were harvested using 0.25% trypsin/EDTA (Gibco, Grand Island, NY, USA) at approximately 80% confluence. The cells were resuspended at 1×10^7 cells/mL in 1 mL of basal medium, and the cell suspension was injected through the renal artery and ureter. The recellularized scaffolds were placed in a sterile incubator at 37 °C overnight. After 10 h, the circulatory perfusion system was re-covered with culture medium, simultaneously introducing sterilized standard equilibrium gas (5% CO_2 and 95% air) into the medium. After coculturing for 10 days, the recellularized kidney scaffolds were harvested. The same method was used to perfuse IM cells into the ureter and renal artery.

2.12 Statistical analysis

Statistical analysis was performed using SPSS 16.0 software. Student's t test was applied for comparisons between independent samples. $P < 0.05$ was considered to indicate statistical significance. The data are expressed as the mean ± standard deviation.

3 Results

3.1 Isolation and identification of ADSCs

ADSCs appeared spindle-like under a microscope (Fig. 1A), and no noticeable differences were observed between cells at passages 1, 3, and 5. After 14 days of adipogenic induction, Oil Red O staining showed red lipid droplets (Fig. 1B). After 21 days of osteogenic induction, the cells stained positively for alizarin red (Fig. 1C). Furthermore, after 21 days of chondrogenic induction, the chondrogenic pellets displayed strong Toluidine Blue staining (Fig. 1D). These tests demonstrated that the ADSCs possessed the ability to differentiate into adipocyte, osteoblasts and chondrocytes. Flow cytometry analysis of the cell phenotype indicated that the percentages of CD29,
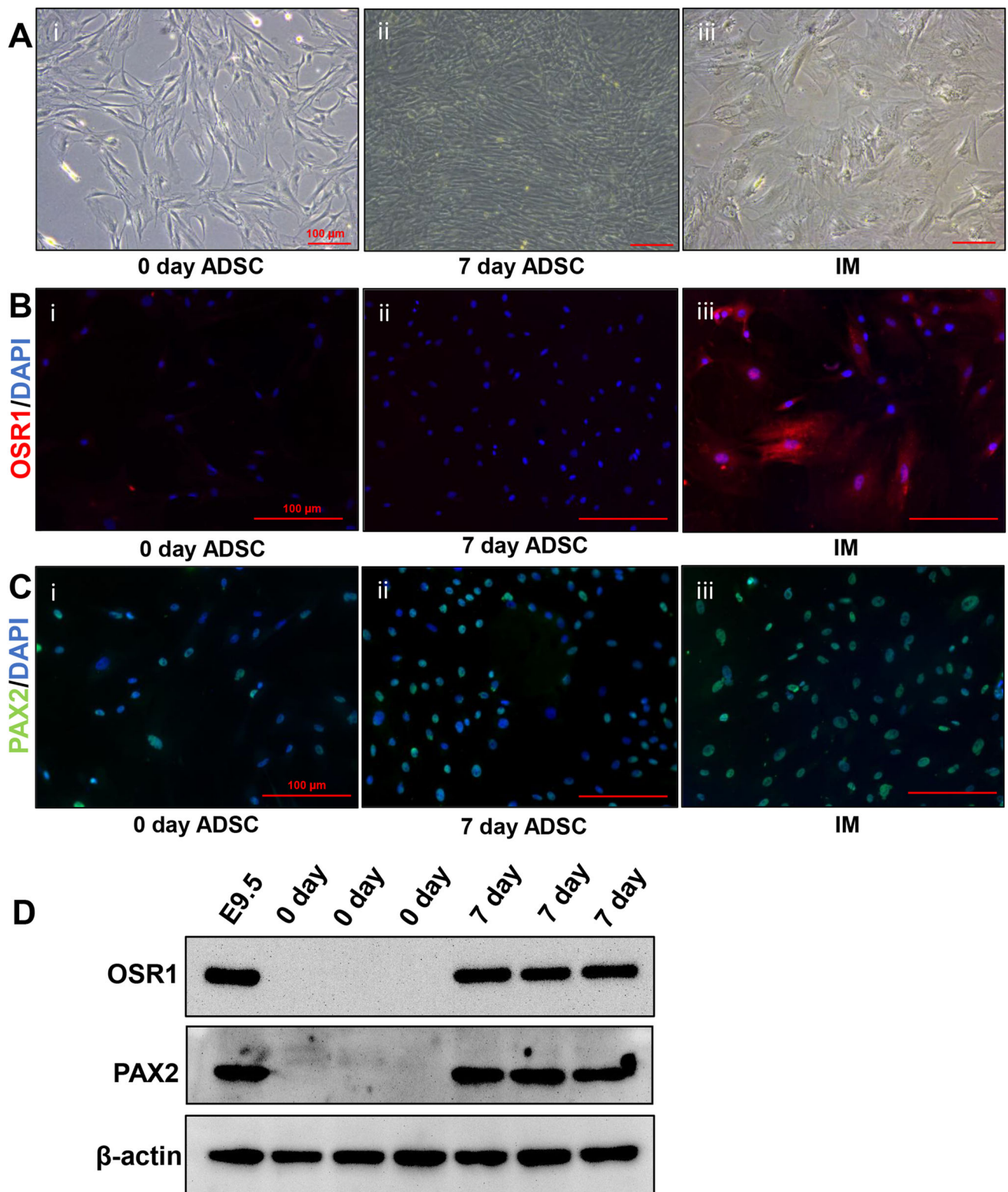
Fig. 2 Inducing ADSCs to differentiate into IM cells. **A** Histology examination of ADSCs and IM cells: Uninduced ADSCs at 0 days (Ai); Uninduced ADSCs at 7 days (Aii); IM cells (Aiii). **B** Immunofluorescence for OSR1: in ADSCs at 0 days (Bi); ADSCs cultured at 7 days (Bii); and IM cells (Biii). **C** Immunofluorescence of PAX2: in ADSCs at 0 days (Ci); ADSCs cultured at 7 days (Cii); and IM cells (Ciii). The scale bar is 100 μm. **D** Western blotting for the expression of PAX2 and OSR1 in ADSCs and IM cells. Mouse embryos at day 9.5 (E9.5) were used as a positive control. PAX2 and OSR1 were not expressed in ADSCs but were highly expressed in E9.5 and IM cells induced from ADSCs

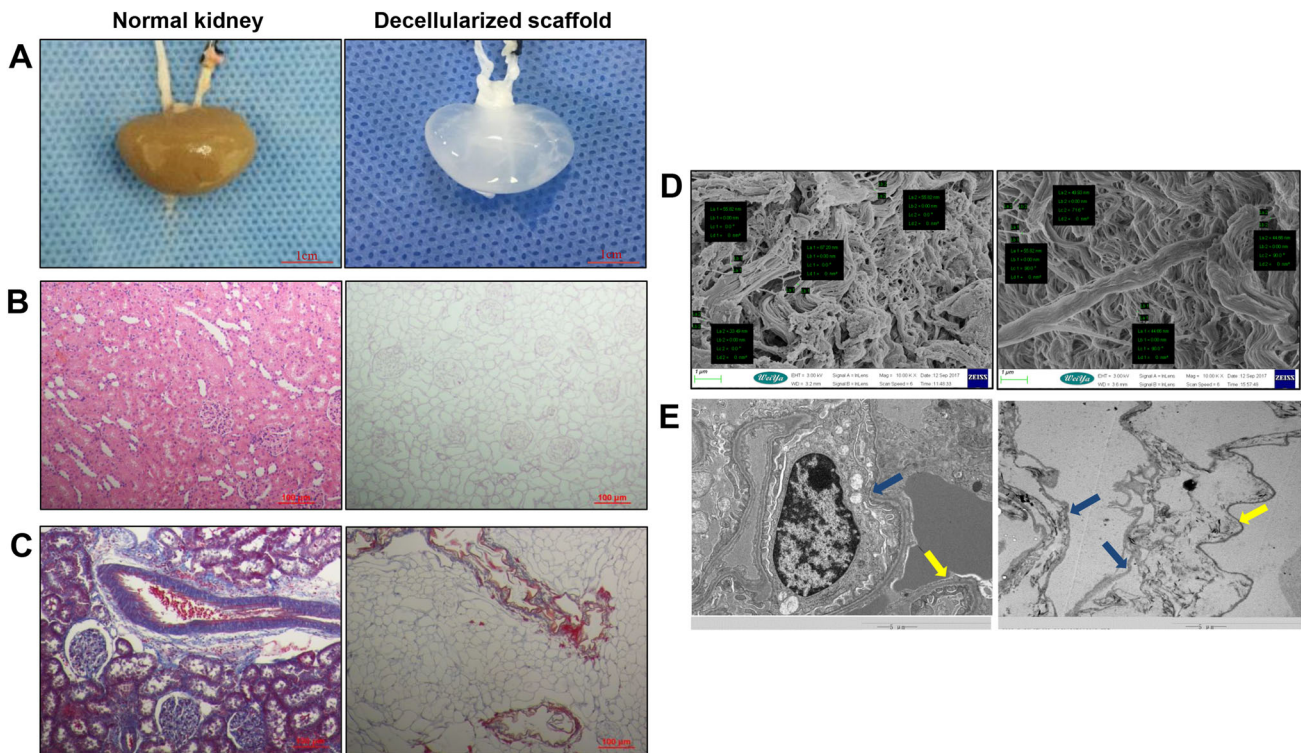**Normal kidney**   **Decellularized scaffold**

Fig. 3 Decellularization of the rat kidney. **A** Photograph of harvested kidney with arterial and ureteral cannulae (left). Harvested kidneys became transparent after decellularization (right). Scale bar is 1 cm. **B** H&E staining of the normal kidney before (left) and after decellularization (right). **C** Masson's trichrome staining of normal kidney (left) and DC scaffold (right). Scale bar is 100 μm. **D** Scanning electron microscopy of normal kidney (left) and DC scaffold (right).

CD90, CD105, CD34, and CD45 were 99.9%, 100%, 97.2%, 1.1%, and 2.4%, respectively (Fig. 1E). The identified cells were used for the subsequent experiments.

3.2 Induction of ADSCs into IM cells and their identification

ADSCs were induced *in vitro* by CHIR99021, an inhibitor of glycogen synthase kinase-3b, and FGF9, for 7 days (Fig. 2A); we then performed immunofluorescence assays to identify OSR1 and PAX2, which are IM-specific markers, and obtained positive results (Fig. 2B, C). Western blotting detection of the protein expression of OSR1 and PAX2 showed the same results (Fig. 2D), indicating that ADSCs were successfully induced into IM cells, which were subsequently combined with DC scaffolds.

3.3 DC scaffolds retained normal renal structure and 3D microstructure

After 6 h of perfusion with 0.5% SDS through the renal artery, the kidney became nearly transparent (Fig. 3A).

The fiber diameter was not significantly different between the DC scaffolds and kidneys ($p > 0.05$, n = 5). The scale bar is 1 μm. **E** Transmission electron microscopy show that the decellularization protocol removed all cell components; the continuity of the basement membrane remained intact. (*Blue arrows* indicate the membrane of Bowman's capsule; a *yellow arrow* indicates the basement membrane of the glomerular capillaries). The scale bar is 5 μm

H&E staining showed that the DC scaffolds were devoid of nuclei and that normal renal structure was retained (Fig. 3B). Masson's trichrome staining showed no cells in the DC scaffolds, and extracellular matrix collagen was retained well compared with normal kidneys. (Figure 3C). Scanning electron microscopy showed that the fiber diameter was not significantly different between the DC scaffolds and kidneys, there had no cell component. ($p > 0.05$, n = 5) (Fig. 3D). Transmission electron microscopy showed that the fiber network of DC scaffolds was maintained well, as indicated by the presence of Bowman's capsule, glomerular capillaries, and mesangial matrix (Fig. 3E).

3.4 Statistical analysis of DNA content, collagen content, and cytokine expression in DC scaffolds

The DC kidney scaffolds showed approximately 95% less DNA compared with normal renal tissues, $p < 0.01$, n = 10 (Fig. 4A); thus, they can be used as recellularized DC scaffolds and combined with IM cells and ADSCs. The collagen content in the DC scaffolds was similar to that in

normal kidneys, $p > 0.05$, n = 10 (Fig. 4B). Moreover, ELISA showed no significant difference in the expression of HGF, VEGF, or TGF-β between the DC scaffolds and native kidney, $p > 0.05$, n = 10 (Fig. 4C–E). Collagen and these cytokines are important for the adherence and further differentiation of stem cells in DC scaffolds.

3.5 Seeded ADSCs attached and differentiated in DC scaffolds

Through renal artery and ureter injection, ADSCs were combined with DC scaffolds after coculture for 10 days. H&E staining revealed that cells were distributed in the vessel, glomerulus and tubule (Fig. 5A). Through renal artery and ureter injection, IM cells were induced by ADSC coculture for 10 days. H&E staining also showed cells attached to the vessel, glomerulus and tubule (Fig. 5B). Immunofluorescent expression of WT1 (a marker of podocytes), E-CAD (a marker of tubules), and GATA3 (a marker of tubules) in the injected ADSCs was negative,

Fig. 5 Recellularization of kidney scaffolds with ADSCs and IM▶ cells. **A** H&E staining of ADSCs seeded into DC scaffolds showed homogeneous distribution of cells in the glomerulus, vascular structures, and tubules. H&E staining shows the gross appearance (left), the glomerular region (middle) and renal tubule (right). **B** IM cells were seeded through the artery and ureter to recellularize the scaffold. H&E staining shows the gross appearance (left), the glomerular region (middle) and renal tubule (right). **C** Immunofluorescence staining for the expression of E-CAD; **D** Immunofluorescence staining for the expression of GATA3; **E** Immunofluorescence staining for the expression of WT1. ADSCs cultured with DC scaffolds for 10 days (i); IM cells cultured with DC scaffolds for 10 days (ii); ADSCs cultured *in vitro* (negative results) (iii); and IM cells cultured *in vitro* (negative results) (iv). The scale bar is 100 μm

whereas positive expression of these proteins was observed in the injected IM cells. This phenomenon was not observed in ADSCs and IM cells cultured *in vitro* (Fig. 5C–E).
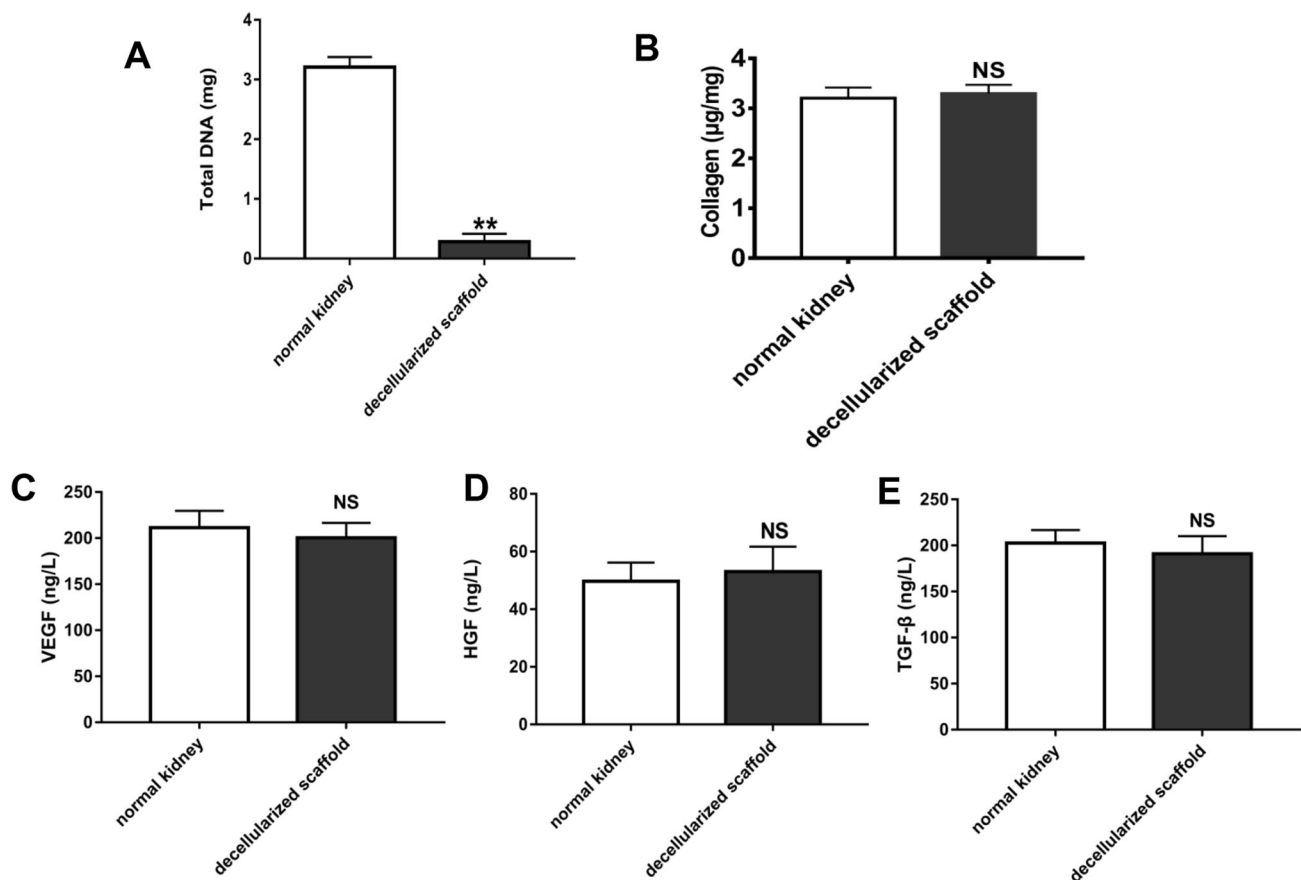

Fig. 4 Quantitative assay for DNA collagen and cytokine levels in DC kidney scaffolds. **A** Biochemical quantification of DNA, **B** and total collagen in normal and DC rat kidney tissue showing a reduction in DNA content ($p < 0.01$) and maintenance of collagen ($p > 0.05$) after perfusion decellularization. **C** The levels of HGF, **D** TGF-b, **E** and VEGF in the DC kidney were not significantly different from those in the native kidney ($p > 0.05$). **$p < 0.01$, NS $p > 0.05$, n = 10. Data are shown as the mean ± standard deviation. Statistical significance ($p < 0.05$) was determined by Student's *t* test
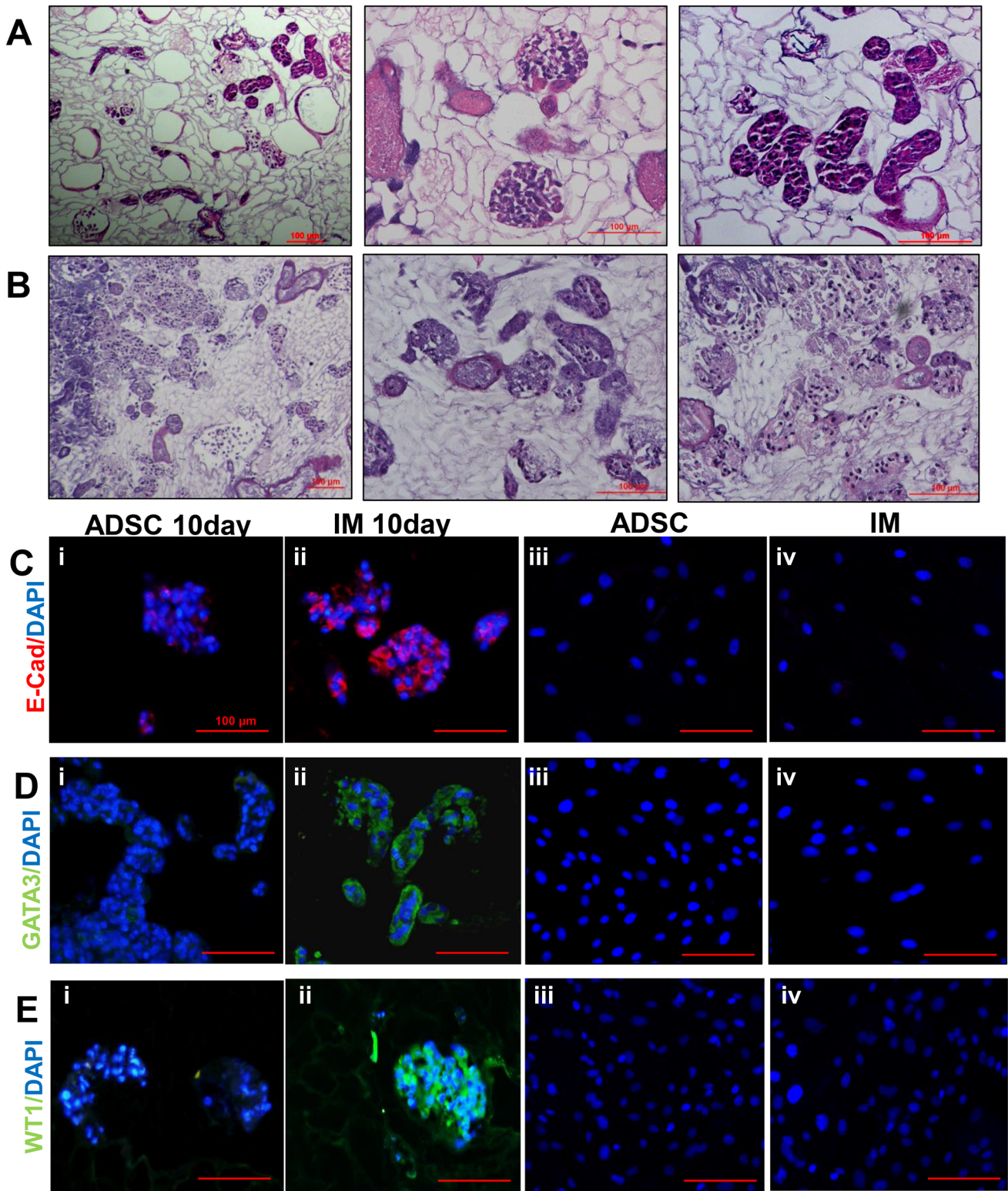
4 Discussion

In this study, IM cells induced from ADSCs were seeded to achieve kidney regeneration, and after 10 days of coculture with DC scaffolds, cell adhesion and differentiation were observed. Immunofluorescence showed that IM cells induced from ADSCs differentiated into tubular and podocyte-like cells in DC scaffolds with higher differentiation efficiency than ADSCs in scaffolds. This phenomenon was not observed in IM cells cultured in vitro. The results further demonstrated that differentiation occurred after the induction of stem cells and that the induced cells had higher differentiation efficiency than the original stem cells. Moreover, DC scaffolds have the ability to induce stem cell differentiation and can be used as an ideal biomaterial for organ regeneration [29–31].

In previous studies, stem cell adhesion was observed in scaffolds, but they did not generate kidney progenitors or mature renal cells [32]. In our study, markers of kidney tubules and podocytes were expressed, signifying the first step in achieving kidney regeneration.

Kidney reconstruction using DC scaffolds and stem cells is a promising strategy for ESRD treatment. Whole-organ perfusion with DC scaffolds and IM cells offers a strategy for regenerative medicine, and our research demonstrated that recellularization of renal scaffolds is possible. Decellularized organs provide the detailed three-dimensional structure required for rebuilding a kidney. In this regard, kidney scaffolds provide a natural substrate and biological and mechanical support to facilitate cell growth and to attract and support cells during tissue regeneration. In addition, scaffolds containing embedded growth factors are used in tissue regeneration, and many of these growth factors are also involved in embryonic development and organogenesis [33, 34]. All of these factors may affect further stem cell differentiation.

ADSCs have the capacity to differentiate in multiple directions with lower potential tumorigenicity. IM cells induced from ADSCs were more stable than ESCs and hiPSC, and they have significant advantages compared with other stem cells, such as abundance, ease of culture, a lack of immunological rejection, multidirectional differentiation across germ layers, and a rapid proliferation rate. ADSCs develop from the mesoderm and can differentiate into various lineages under the stimulation of specific growth factors and environmental induction. Notably, ADSCs have been confirmed to be induced to differentiate into osteoblasts [19], adipocytes [20], chondrocytes [21], endoderm-derived hepatocytes [35], islet β-like cells [36], ectoderm-derived neurons [37], cardiomyocytes [38], and epidermal cells [39]. In our experiments, we successfully

induced ADSCs into IM cells and combined them with DC scaffolds.

Previous studies showed that stem cells could be combined with DC scaffolds, but their differentiation in the scaffolds was not shown, as no kidney cell-specific markers were used [14, 27, 32]. We attempted to induce ADSCs into IM cells and combine them with DC scaffolds to construct a regenerated kidney. As a result, IM cell differentiation was observed in the DC scaffolds. To the best of our knowledge, this study is the first to show the induction of ADSCs into IM cells and the subsequent combination with DC scaffolds. We speculate that this phenomenon of differentiation may be due to the factors in specific signaling pathways that affect stem cells at different stages of differentiation, such as the glial cell line-derived neurotrophic factor (GDNF)/Ret and Wnt signaling pathways. GDNF is secreted by the metanephric mesenchyme and is necessary for outgrowth of the ureteric bud (UB) and subsequent UB branching morphogenesis through the GDNF/Ret signaling pathway [40–42]. Wnt4 is expressed in the metanephric mesenchyme, and Wnt signaling is essential for nephron progenitors to undergo a mesenchymal-to-epithelial transition in the early phases of nephrogenesis [43–45]. This finding forms the basis of our future investigations. DC scaffolds retained cytokines such as HGF, TGF-β, and VEGF, but the level of cytokines required to induce direct stem cell differentiation was insufficient. ADSCs are able to undergo multidirectional differentiation. Because it is difficult to control the direction of ADSC differentiation in DC scaffolds, we adopted the strategy of combining IM cells induced from ADSCs in vitro with DC scaffolds. The results showed that the differentiation efficiency of IM cells in DC scaffolds into tubular and podocyte-like cells was higher than that of ADSCs. The combination of stem cells with DC scaffolds to achieve kidney regeneration is a potentially ideal strategy for ESRD treatment. DC scaffolds have the feature of low immunogenicity and are suitable for transplantation, while stem cells could be harvested from patients and have the capability of multidirectional differentiation in vitro.

In this study, we induced ADSCs to specific stages and combined them with DC scaffolds. After coculture with the scaffolds, ADSCs continued to differentiate into the DC scaffolds and expressed markers of kidney cells. Notably, this phenomenon could not be observed for untreated ADSCs in the DC scaffolds, which supported recellularized kidney cell growth but limited ADSC differentiation. Furthermore, we have identified that ADSC cells could be induced into intermediate mesoderm.

There are some limitations to this study. First, the quantity of cells in the DC scaffolds was insufficient, and the efficiency of cell differentiation was not satisfactory. Therefore, the regenerated kidney cannot display full

kidney function. Second, the nutrition supply in the recellularized scaffolds has not been resolved, which may influence the differentiation of cells and the function of the recellularized kidney. Last, in this study, throughout the process of ADSC differentiation in DC scaffolds, the signaling pathways affecting the ADSCs remain unclear, and additional studies are needed. This research will be performed in our subsequent studies. Once these problems are solved, our developed strategy will undoubtedly become a potential solution for patients suffering from kidney diseases.

In conclusion, we have shown that induced intermediate mesoderm cells in decellularized scaffolds could have higher differentiation efficiency than the original stem cells. Intermediate mesoderm cells grow well and differentiate toward tubular-like cells and podocyte-like cells. Therefore, inducing stem cell differentiation with scaffolds is a feasible strategy for renal regeneration. DC scaffolds have the ability to induce stem cell differentiation and could be used as an ideal biomaterial for kidney regeneration.

Compliance with ethical standards

Conflict of interest All authors declare that there is no conflict of interest.

Ethical statement This study was approved by the Animal Ethics Committee of Shandong University [KYLL-2017(GJ)A-0011]. All surgical procedures were performed according to the Guide for the Care and Use of Laboratory Animals.

References

1. Liyanage T, Ninomiya T, Jha V, Neal B, Patrice HM, Okpechi I, et al. Worldwide access to treatment for end-stage kidney disease: a systematic review. Lancet. 2015;385:1975–82.
2. Luan FL, Steffick DE, Ojo AO. Steroid-free maintenance immunosuppression in kidney transplantation: is it time to consider it as a standard therapy. Kidney Int. 2009;76:825–30.
3. Wolfe RA, Ashby VB, Milford EL, Ojo AO, Ettenger RE, Agodoa LY, et al. Comparison of mortality in all patients on dialysis, patients on dialysis awaiting transplantation, and recipients of a first cadaveric transplant. N Engl J Med. 1999;341:1725–30.
4. Jha V, Garcia-Garcia G, Iseki K, Li Z, Naicker S, Plattner B, et al. Chronic kidney disease: global dimension and perspectives. Lancet. 2013;382:260–72.
5. Yamanaka S, Yokoo T. Current bioengineering methods for whole kidney regeneration. Stem Cells Int. 2015;2015:724047.
6. Gomes ME, Rodrigues MT, Domingues RMA, Reis RL. Tissue engineering and regenerative medicine: new trends and directions-a year in review. Tissue Eng Part B Rev. 2017;23:211-24.
7. Usui J, Kobayashi T, Yamaguchi T, Knisely AS, Nishinakamura R, Nakauchi H. Generation of kidney from pluripotent stem cells via blastocyst complementation. Am J Pathol. 2012;180:2417–26.
8. Hinata N, Suzuki R, Ishizawa A, Miyake H, Rodriguez-Vazquez JF, Murakami G, et al. Fetal development of the mesonephric artery in humans with reference to replacement by the adrenal and renal arteries. Ann Anat. 2015;202:8–17.
9. Takasato M, Er PX, Chiu HS, Maier B, Baillie GJ, Ferguson C, et al. Kidney organoids from human iPS cells contain multiple lineages and model human nephrogenesis. Nature. 2015;526:564–8.
10. Humes HD, MacKay SM, Funke AJ, Buffington DA. Tissue engineering of a bioartificial renal tubule assist device: in vitro transport and metabolic characteristics. Kidney Int. 1999;55:2502–14.
11. Song JJ, Ott HC. Organ engineering based on decellularized matrix scaffolds. Trends Mol Med. 2011;17:424–32.
12. Lelongt B, Ronco P. Role of extracellular matrix in kidney development and repair. Pediatr Nephrol. 2003;18:731–42.
13. Sullivan DC, Mirmalek-Sani SH, Deegan DB, Baptista PM, Aboushwareb T, Atala A, et al. Decellularization methods of porcine kidneys for whole organ engineering using a high-throughput system. Biomaterials. 2012;33:7756–64.
14. Sambi M, Chow T, Whiteley J, Li M, Chua S, Raileanu V, et al. Acellular mouse kidney ECM can be used as a three-dimensional substrate to test the differentiation potential of embryonic stem cell derived renal progenitors. Stem Cell Rev. 2017;13:513–31.
15. Ross EA, Williams MJ, Hamazaki T, Terada N, Clapp WL, Adin C, et al. Embryonic stem cells proliferate and differentiate when seeded into kidney scaffolds. J Am Soc Nephrol. 2009;20:2338–47.
16. Figliuzzi M, Bonandrini B, Remuzzi A. Decellularized kidney matrix as functional material for whole organ tissue engineering. J Appl Biomater Funct Mater. 2017;15:e326–33.
17. Chani B, Puri V, Sobti RC, Jha V, Puri S. Decellularized scaffold of cryopreserved rat kidney retains its recellularization potential. PLoS One. 2017;12:e0173040.
18. Zuk PA, Zhu M, Ashjian P, De Ugarte DA, Huang JI, Mizuno H, et al. Human adipose tissue is a source of multipotent stem cells. Mol Biol Cell. 2002;13:4279–95.
19. Sollazzo V, Lucchese A, Palmieri A, Zollino I, Iaccarino C, Carnevali G, et al. Polylactide-polyglycolide resorbable plates stimulates adipose tissue-derived stem cells towards osteoblasts differentiation. Int J Immunopathol Pharmacol. 2011;24:59–64.
20. Lee J, Abdeen AA, Tang X, Saif TA, Kilian KA. Matrix directed adipogenesis and neurogenesis of mesenchymal stem cells derived from adipose tissue and bone marrow. Acta Biomater. 2016;42:46–55.
21. Huang SJ, Fu RH, Shyu WC, Liu SP, Jong GP, Chiu YW, et al. Adipose-derived stem cells: isolation, characterization, and differentiation potential. Cell Transplant. 2013;22:701–9.
22. Guan Y, Liu S, Sun C, Cheng G, Kong F, Luan Y, et al. The effective bioengineering method of implantation decellularized renal extracellular matrix scaffolds. Oncotarget. 2015;6:36126–38.
23. Xue A, Niu G, Chen Y, Li K, Xiao Z, Luan Y, et al. Recellularization of well-preserved decellularized kidney scaffold using adipose tissue-derived stem cells. J Biomed Mater Res A. 2018;106:805–14.

24. Zhu Y, Liu T, Song K, Fan X, Ma X, Cui Z. Adipose-derived stem cell: a better stem cell than BMSC. Cell Biochem Funct. 2008;26:664–75.

25. Xu LJ, Wang SF, Wang DQ, Ma LJ, Chen Z, Chen QQ, et al. Adipose-derived stromal cells resemble bone marrow stromal cells in hepatocyte differentiation potential in vitro and in vivo. World J Gastroenterol. 2017;23:6973–82.

26. Xie X, Du X, Li K, Chen Y, Guan Y, Zhao X, et al. Construction of engineered corpus cavernosum with primary mesenchymal stem cells in vitro. Sci Rep. 2017;7:18053.

27. O'Neill JD, Freytes DO, Anandappa AJ, Oliver JA, Vunjak-No-vakovic GV. The regulation of growth and metabolism of kidney stem cells with regional specificity using extracellular matrix derived from kidney. Biomaterials. 2013;34:9830–41.

28. Takasato M, Little MH. Making a kidney organoid using the directed differentiation of human pluripotent stem cells. Methods Mol Biol. 2017;1597:195–206.

29. Santi PA, Johnson SB. Decellularized ear tissues as scaffolds for stem cell differentiation. J Assoc Res Otolaryngol. 2013;14:3–15.

30. Perniconi B, Coletti D, Aulino P, Costa A, Aprile P, Santacroce L, et al. Muscle acellular scaffold as a biomaterial: effects on C2C12 cell differentiation and interaction with the murine host environment. Front Physiol. 2014;5:354.

31. Zhang W, Huo Y, Wang X, Jia Y, Su L, Wang C, et al. Decel-lularized ovine arteries as biomatrix scaffold support endothelial of mesenchymal stem cells. Heart Vessels. 2016;31:1874–81.

32. Bonandrini B, Figliuzzi M, Papadimou E, Morigi M, Perico N, Casiraghi F, et al. Recellularization of well-preserved acellular kidney scaffold using embryonic stem cells. Tissue Eng Part A. 2014;20:1486–98.

33. Brown BN, Badylak SF. Extracellular matrix as an inductive scaffold for functional tissue reconstruction. Transl Res. 2014;163:268–85.

34. Clause KC, Barker TH. Extracellular matrix signaling in mor-phogenesis and repair. Curr Opin Biotechnol. 2013;24:830–3.

35. Lee HJ, Jung J, Cho KJ, Lee CK, Hwang SG, Kim GJ. Com-parison of in vitro hepatogenic differentiation potential between various placenta-derived stem cells and other adult stem cells as an alternative source of functional hepatocytes. Differentiation. 2012;84:223–31.

36. Sun Y, Zhang M, Ji S, Liu L. Induction differentiation of rabbit adiposederived stromal cells into insulinproducing cells in vitro. Mol Med Rep. 2015;12:6835–40.

37. Zhang HT, Liu ZL, Yao XQ, Yang ZJ, Xu RX. Neural differ-entiation ability of mesenchymal stromal cells from bone marrow and adipose tissue: a comparative study. Cytotherapy. 2012;14:1203–14.

38. Choi YS, Dusting GJ, Stubbs S, Arunothayaraj S, Han XL, Collas P, et al. Differentiation of human adipose-derived stem cells into beating cardiomyocytes. J Cell Mol Med. 2010;14:878–89.

39. Lu W, Yu J, Zhang Y, Ji K, Zhou Y, Li Y, et al. Mixture of fibroblasts and adipose tissue-derived stem cells can improve epidermal morphogenesis of tissue-engineered skin. Cells Tissues Organs. 2012;195:197–206.

40. Costantini F, Shakya R. GDNF/Ret signaling and the develop-ment of the kidney. Bioessays. 2006;28:117–27.

41. Tang MJ, Cai Y, Tsai SJ, Wang YK, Dressler GR. Ureteric bud outgrowth in response to RET activation is mediated by phos-phatidylinositol 3-kinase. Dev Biol. 2002;243:128–36.

42. Kuure S, Sainio K, Vuolteenaho R, Ilves M, Wartiovaara K, Immonen T, et al. Crosstalk between Jagged1 and GDNF/Ret/ GFRalpha1 signalling regulates ureteric budding and branching. Mech Dev. 2005;122:765–80.

43. Schmidt-Ott KM, Masckauchan TN, Chen X, Hirsh BJ, Sarkar A, Yang J, et al. beta-catenin/TCF/Lef controls a differentiation-associated transcriptional program in renal epithelial progenitors. Development. 2007;134:3177–90.

44. Park JS, Valerius MT, McMahon AP. Wnt/beta-catenin signaling regulates nephron induction during mouse kidney development. Development. 2007;134:2533–9.

45. Stark K, Vainio S, Vassileva G, McMahon AP. Epithelial trans-formation of metanephric mesenchyme in the developing kidney regulated by Wnt-4. Nature. 1994;372:679–83.